International Journal of
Molecular Sciences

MDPI

Article

Excess BAFF Alters NR4As Expression Levels and Breg Function of Human Precursor-like Marginal Zone B-Cells in the Context of HIV-1 Infection

Kim Doyon-Laliberté [1,2,†], Matheus Aranguren [1,2,†], Michelle Byrns [1,2], Josiane Chagnon-Choquet [1,2], Matteo Paniconi [3], Jean-Pierre Routy [4], Cécile Tremblay [1,2], Marie-Claude Quintal [5], Nathalie Brassard [1,2], Daniel E. Kaufmann [1,6], Johanne Poudrier [1,2,*,‡] and Michel Roger [1,2,*,‡]

1 Centre de Recherche du Centre Hospitalier de l'Université de Montréal (CRCHUM), Montréal, QC H2X 0A9, Canada
2 Département de Microbiologie, Infectiologie et Immunologie de l'Université de Montréal, Montréal, QC H3T 1J4, Canada
3 Service d'Aide à la Formation Interdisciplinaire et à la Réussite Étudiante (SAFIRE), Faculté des Arts et Sciences de l'Université de Montréal, Montréal, QC H3T 1N8, Canada
4 Department of Medicine, McGill University Health Centre, McGill University, Montréal, QC H4A 3J1, Canada
5 Centre Hospitalier Ste-Justine de l'Université de Montréal, Montréal, QC H3T 1C5, Canada
6 Département de Médecine de l'Université de Montréal, Montréal, QC H3T 1J4, Canada
* Correspondence: johanne.poudrier@umontreal.ca (J.P.); michel.roger.chum@ssss.gouv.qc.ca (M.R.)
† These authors contributed equally to this work.
‡ These authors contributed equally to this work.

Citation: Doyon-Laliberté, K.; Aranguren, M.; Byrns, M.; Chagnon-Choquet, J.; Paniconi, M.; Routy, J.-P.; Tremblay, C.; Quintal, M.-C.; Brassard, N.; Kaufmann, D.E.; et al. Excess BAFF Alters NR4As Expression Levels and Breg Function of Human Precursor-like Marginal Zone B-Cells in the Context of HIV-1 Infection. *Int. J. Mol. Sci.* **2022**, *23*, 15142. https://doi.org/10.3390/ijms232315142

Academic Editor: Agustín Valenzuela-Fernández

Received: 9 November 2022
Accepted: 29 November 2022
Published: 1 December 2022

Abstract: We have reported excess B-cell activating factor (BAFF) in the blood of HIV-infected progressors, which was concomitant with increased frequencies of precursor-like marginal zone (MZp) B-cells, early on and despite antiretroviral therapy (ART). In controls, MZp possess a strong B-cell regulatory (Breg) potential. They highly express IL-10, the orphan nuclear receptors (NR)4A1, NR4A2 and NR4A3, as well as the ectonucleotidases CD39 and CD73, all of which are associated with the regulation of inflammation. Furthermore, we have shown MZp regulatory function to involve CD83 signaling. To address the impact of HIV infection and excessive BAFF on MZp Breg capacities, we have performed transcriptomic analyses by RNA-seq of sorted MZp B-cells from the blood of HIV-infected progressors. The Breg profile and function of blood MZp B-cells from HIV-infected progressors were assessed by flow-cytometry and light microscopy high-content screening (HCS) analyses, respectively. We report significant downregulation of NR4A1, NR4A2, NR4A3 and CD83 gene transcripts in blood MZp B-cells from HIV-infected progressors when compared to controls. NR4A1, NR4A3 and CD83 protein expression levels and Breg function were also downregulated in blood MZp B-cells from HIV-infected progressors and not restored by ART. Moreover, we observe decreased expression levels of NR4A1, NR4A3, CD83 and IL-10 by blood and tonsillar MZp B-cells from controls following culture with excess BAFF, which significantly diminished their regulatory function. These findings, made on a limited number of individuals, suggest that excess BAFF contributes to the alteration of the Breg potential of MZp B-cells during HIV infection and possibly in other situations where BAFF is found in excess.

Keywords: HIV; Breg; NR4A; MZp; BAFF

1. Introduction

Currently, over 37 million individuals are living with the human immunodeficiency virus (HIV) [1]. Although over 66% of these individuals are successfully treated with antiretroviral therapy (ART), inflammation persists [1,2]. Consistently, we have previously reported that expression levels of the tumor necrosis factor (TNF) family member B-cell Activating Factor (BAFF, TNFSF13B) are in excess in the blood of HIV-infected progressors

from the Montreal Primary HIV Infection (PHI) cohort. This upregulation is already present in the acute phase of infection and is still observed 9–12 months post-ART [3]. Moreover, our recent studies suggest that excess BAFF perseveres in progressors on ART for more than 15 years of the Canadian HIV and Aging Cohort Study (CHACS) [4]. Excess BAFF is associated with viral factors, such as Nef, and non-viral factors, such as elements of microbial translocation, and correlates with hypergammaglobulinemia and dysregulation of the B-cell compartment [5–7]. BAFF is an important growth factor that helps shape the marginal zone (MZ) B-cell pool. As such, we found that excess BAFF is associated with increased frequencies of a $CD19^{+}CD1c^{+}CD21^{lo}IgM^{hi}CD27^{+}CD10^{+}$ B-cell population, sharing features of transitional immature and MZ B-cells, we designated "Precursor-like" Marginal Zone (MZp) B-cells, in the blood of PHI progressors [3], and more recently in the blood of CHACS participants [4]. We have reported similar observations with HIV-Transgenic (Tg) mice [8], SIV-infected macaques [9] and with HIV-infected Beninese commercial sex workers [10,11], suggesting that excess BAFF and dysregulated MZp B-cells are reliable markers of inflammation and disease progression in the context of HIV.

BAFF binds to three receptors among B-cell subsets: TNF receptor superfamily 13C (TNFRSF13C, BAFFR), TNF receptor superfamily 13B (TNFRSF13B, TACI) and TNF receptor superfamily 17 (TNFRSF17, BCMA), the second of which is highly expressed by MZ populations [12]. MZ are first-line B-cells that respond quickly to blood-borne antigens via their polyreactive BcR (IG + CD79) and numerous Pattern Recognition Receptors (PRR) such as C-type lectins and Toll-like Receptors (TLR). MZ B-cells have been shown to class-switch their immunoglobulins (IG) from IgM to IgG or IgA in a BAFF-dependent manner via TACI [12]. Importantly, MZ B-cells were shown to bind to the envelope (Env) proteins gp120 and gp41 of HIV, via C-type lectins and TLR10, respectively [13,14]. Whether IG produced by MZ B-cells confer some level of protection or contribute to hyperglobulinemia and autoimmune manifestations in excessive BAFF contexts, such as with HIV, is currently under investigation.

Importantly, we have recently reported that in controls, blood and tonsil MZp B-cells present features associated with strong B-cell regulatory (Breg) capacities [15]. Indeed, transcriptomic and flow-cytometry analyses demonstrated that MZp B-cells express high levels of interleukin 10 (IL-10), interleukin 35 (IL12A, IL35 subunit) and transforming growth factor beta 1 (TGFB1, TGFβ), as well as the ectonucleotidases ENTPD1 (ectonucleoside triphosphate diphosphohydrolase 1, CD39) and NT5E (5′-nucleotidase ecto, CD73). Strikingly, as for regulatory T-cells (Tregs) [16,17], we found that MZp B-cells highly express the orphan Nuclear Receptors Subfamily 4 Group A Member 1 (NR4A1), NR4A2 and NR4A3, as well as the immunoregulatory molecule CD83 [15], whose expression was shown to be directly modulated by NR4A1, NR4A2 and NR4A3 [18]. Notably, we have shown that the in vitro Breg function of tonsil MZp B-cells involved CD83 signaling [15].

NR4A transcription factors are involved in the regulation of the inflammatory response and their expression is increased upon signaling via the TcR (TR + CD3) or BcR [19], amongst others. They are important regulators of differentiation, proliferation and apoptosis of immune cells [20]. The importance of NR4A transcription factors in immune regulation is highlighted by their importance for Tregs, as NR4A transcription factors directly promote and maintain the expression of FOXP3 [17]. Also, increased expression of NR4A1 in myeloid cells is associated with a diminished T-cell activation profile [21]. Furthermore, NR4A1-3 knockout mice develop systemic autoimmune diseases [20,22].

Given the importance of BAFF for MZ B-cell activity, we have herein assessed the impact of the HIV infection and excess BAFF on the Breg profile and function of MZp B-cells. We show that NR4A1-3 as well as CD83 gene and protein expression levels are severely downregulated in blood MZp B-cells from PHI progressors when compared to controls and HIV-elite controllers (ECs), whose plasma viral load remain undetectable in the absence of ART. Importantly, this downregulation correlates with reduced MZp Breg function. Moreover, this loss of Breg function could be related to the exhaustion profile we describe for this population. We also find that excess BAFF, both as soluble and membrane

forms, directly downregulate NR4A1-3 and CD83 expression levels by MZp from the tonsils of control donors in vitro. Total tonsillar membrane BAFF expression levels were also found to correlate with MZp Breg efficiency, as donors expressing relatively low BAFF levels at baseline had a stronger Breg function than donors who had higher BAFF levels at baseline. Strikingly, adding soluble BAFF was found to impede MZp Breg function in low BAFF-expressing tonsillar donors. Altogether, these results suggest that in circumstances of excess BAFF, alteration of MZp Breg profile and function may constitute a major threat to "immune surveillance". As such, the group of Nus et al. described that depletion of NR4A1 in MZ B-cell populations exacerbated atherosclerosis, thus alluding to the MZ B-cell populations' capacity of "immune surveillance" to prevent atherosclerosis, and possibly other co-morbidities associated with chronic inflammatory conditions [23,24].

2. Results

2.1. Socio-Demographic and Data Characteristics of the Cohorts Used in This Study

Characterizations of the samples from the PHI cohort selected for this study show that there are significant differences for plasma viral loads and blood $CD4^+$ T-cell counts between progressors before and after ART treatment, as expected. No significant difference for age, $CD4^+$ T-cell counts and $CD8^+$ T-cell counts were found between the progressors (5–8 months) and EC (Table 1).

Table 1. Socio-demographic and data characteristics of the cohorts used for the RNAseq and flow cytometry analyses. Statistical analyses were done between samples selected from progressors (HIV+) and elite controllers (EC), and between HIV+ untreated (ART−) and treated (ART+) individuals. Statistical significance of difference in clinical data between progressors before and after ART was assessed with the Wilcoxon matched-pairs test. Statistical significance of difference between progressors and EC was assessed with the Mann–Whitney U test. [1] Undetectable viral loads were found in the three ECs.

	RNA-Seq Analysis			Flow-Cytometry Analysis		
Group	**HIV+ (n = 3)**	**EC (n = 3)**	**p-Value**	**HIV+ ART− (n = 10)**	**HIV+ ART+ (n = 10)**	**p-Value**
Age	38.67 (28–44)	38.67 (37–40)	0.7	NA	NA	NA
Viral load	213,353 (51,045–418,465)	NA [1]	NA	1,258,139 (374–6,193,724)	41.4 (20–234)	0.002
$CD4^+$ T-cell count (cells/mm^3)	540 (380–760)	819 (737–920)	0.2	447 (284–590)	776.5 (565–1210)	0.0006
$CD8^+$ T-cell count (cells/mm^3)	871–(520–1153)	821 (303–1130)	>0.99	1128 (0–3190)	634.3 (210–1080)	0.06
ART duration (weeks)	NA	NA	NA	NA	92 (84–96)	NA

2.2. Blood MZp B-Cells from Progressors Show An Altered Transcriptomic Profile

We have previously shown that progressors from the Montreal PHI cohort presented higher levels of both BAFF and MZp B-cell frequencies in their blood, despite 1 year of ART [3]. To further assess the impact of HIV infection and associated excessive BAFF condition on the dysregulation of MZp, we FACS-sorted MZ and MZp B-cell populations from the blood of three PHI progressors (5–8 months), three ECs and three controls selected from the above-mentioned study [3], and proceeded to transcriptomic analyses by RNA-seq. As depicted in Figure 1, PCA analyses of the top 5000 varying genes show that the gene expression profiles of blood MZ and MZp B-cell populations from the progressors present a distinct pattern when compared to that of both EC and controls, who share greater similarity (Figure 1A). Given this similarity between EC and controls and the scope of this manuscript, we then generated a heat map of the top 100 differently expressed genes (DEG) between blood MZp B-cells of the progressors and controls. We show that among those, Interferon Stimulated Genes (ISG) such as 2′-5′-oligoadenylate synthetase 1 (OAS1) ($p = 3 \times 10^{-6}$), SAM and HD domain-containing deoxynucleoside triphosphate

triphosphohydrolase 1 (SAMHD1) ($p = 5 \times 10^{-6}$) and SP110 nuclear body protein (SP110) ($p = 3 \times 10^{-10}$) are significantly upregulated in MZp from the progressors, whereas genes that have a role in regulation are severely downregulated in MZp from these same individuals (Figures 1B,C and 2). The DEG were also analyzed by a volcano plot, showing that 709 genes are significantly downregulated and 392 are significantly upregulated in blood MZp B-cells from the progressors (Figure 1C) when compared to controls. Gene Set Enrichment Analyses (GSEA) show that both PI3K-AKT-MTOR and CREB/cJUN signatures are downregulated in blood MZp B-cells from the progressors (Figure 1D,E, and Supplementary Figure S2). Accordingly, blood MZp B-cells from the progressors express higher levels of gene transcripts for exhaustion markers such as T-box transcription factor 21 (T-bet, TBX21) ($p = 0.1$), integrin subunit alpha X (CD11c, ITGAX) ($p = 0.009$), FCRL5 ($p = 0.003$), and leukocyte immunoglobulin-like receptor B1 (CD85j, LILRB1) ($p = 0.007$), as well as the negative regulators CD22 ($p = 0.05$) and CD72 ($p = 0.003$) (Figure 1F–K) when compared to blood MZp B-cells from controls. Altogether, these results suggest that HIV disease progression greatly solicits the activities of MZ B-cell populations, which leads to changes in their transcriptomic profile and possibly functional impairment, especially in the MZp B-cell sub-population, which presents signs of exhaustion.

2.3. Blood MZp B-Cells from Progressors Express Lower Levels of Regulatory Markers

Consistent with the severely altered profiles described above, we found highly significant downregulation of gene transcripts for the NR4A family members in blood MZp B-cells of the progressors. Indeed, gene expression levels of NR4A1 ($p = 0.01$), NR4A2 ($p = 3 \times 10^{-9}$), NR4A3 ($p = 1 \times 10^{-36}$), as well as genes that they regulate directly such as CD83 ($p = 3 \times 10^{-9}$) and interleukin 6 (IL-6) (3×10^{-6}) (Figure 2A–E), were very significantly downregulated in blood MZp B-cells from the progressors when compared to that of controls. Given the similarity observed with NR4As gene expression levels of controls and EC, and the scope of this manuscript, further characterization of MZp Breg capacities were conducted with progressors and controls. We next sought to assess whether the transcriptomic downregulation of Breg markers was suggestive of their protein downregulation. To this end, blood samples from 15 controls and 10 progressors (before and after ART) were selected, including samples from the individuals selected for the RNA-seq analyses. We have measured the protein expression levels of the Breg markers NR4A1, NR4A3, CD83, CD39 and CD73 by multicolor flow cytometry on MZp B-cells from the blood of these individuals. As expected, protein expression levels of NR4A1, NR4A3, CD83 and CD73 were downregulated by blood MZp B-cells from progressors when compared to those of controls (Figure 2G–K). Strikingly, ART did not restore expression levels of these Breg markers and some of them, such as NR4A3 and CD83, were further downregulated despite ART (Figure 2L–P). Of note, consistent with previous reports, membrane BAFF levels were found to be in excess in samples from these progressors and were not restored by ART (Figure 2Q–R). Also, as expected, MZp frequencies in the blood of these progressors, without and with ART, were significantly higher compared to that of controls (Figure 2S). However, no significant correlation between MZp frequencies and BAFF levels could be observed for progressors (R: 0.1; p-value 0.95) or after ART treatment (R: 0.3; p-value 0.6833). Of note, the small numbers of samples in our groups did not allow us to reach significance for correlations between blood BAFF levels and MZp frequencies; however, as stated earlier, we have previously reported excess BAFF to be concomitant with increased MZp frequencies in several cohorts and study systems. Our data suggest that MZp Breg capacities may be altered in progressors, regardless of therapy. These data also suggest that excess BAFF might contribute to altering the Breg profile of MZp.

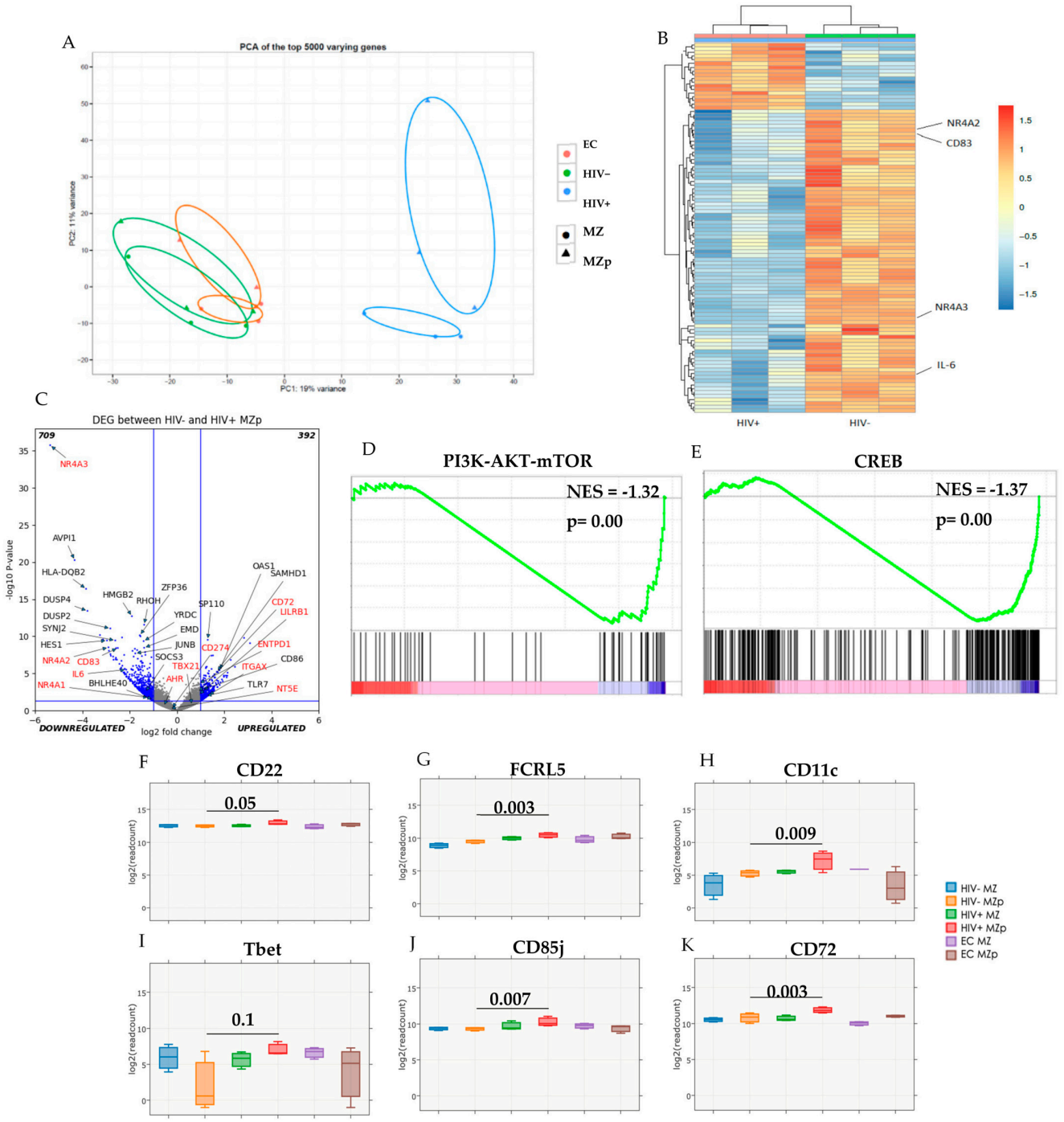

Figure 1. The transcriptomic profile of blood marginal zone (MZ) B-cell populations from progressors is different from that of elite controllers and controls. Data exploration of the transcriptomic analyses by RNAseq of sorted mature marginal zone (MZ) and MZ precursor-like (MZp) B-cells from the blood of 5-8 months progressors (HIV+), elite controllers (EC) and controls (HIV−). Principal Component Analysis (PCA) of the top 5000 genes (**A**). Heat Map of the top 100 Differentially Expressed Genes (DEG) between MZp B-cells from progressors and controls (full-sized Heat Map in Supp. Materials) (**B**). Volcano Plot between blood MZp B-cells from the controls and progressors groups (**C**). Gene Set Enrichment Analyses (GSEA) of PI3K-AKT-MTOR (NES = −1.32, $p < 0.0001$) (**D**) and CREB/cJUN (NES = −1.37, $p < 0.0001$) (**E**) pathways in blood MZp B-cells from progressors when compared to controls. RNAseq analyses of Tbet (**F**), CD11c (**G**), FCRL5 (**H**), CD22 (**I**), CD72 (**J**) and CD85j (**K**) gene expression levels. $n = 3$ for each group of participants. The Wald Test with Benjamini–Hochberg correction was used for RNAseq analysis (**F**–**K**).

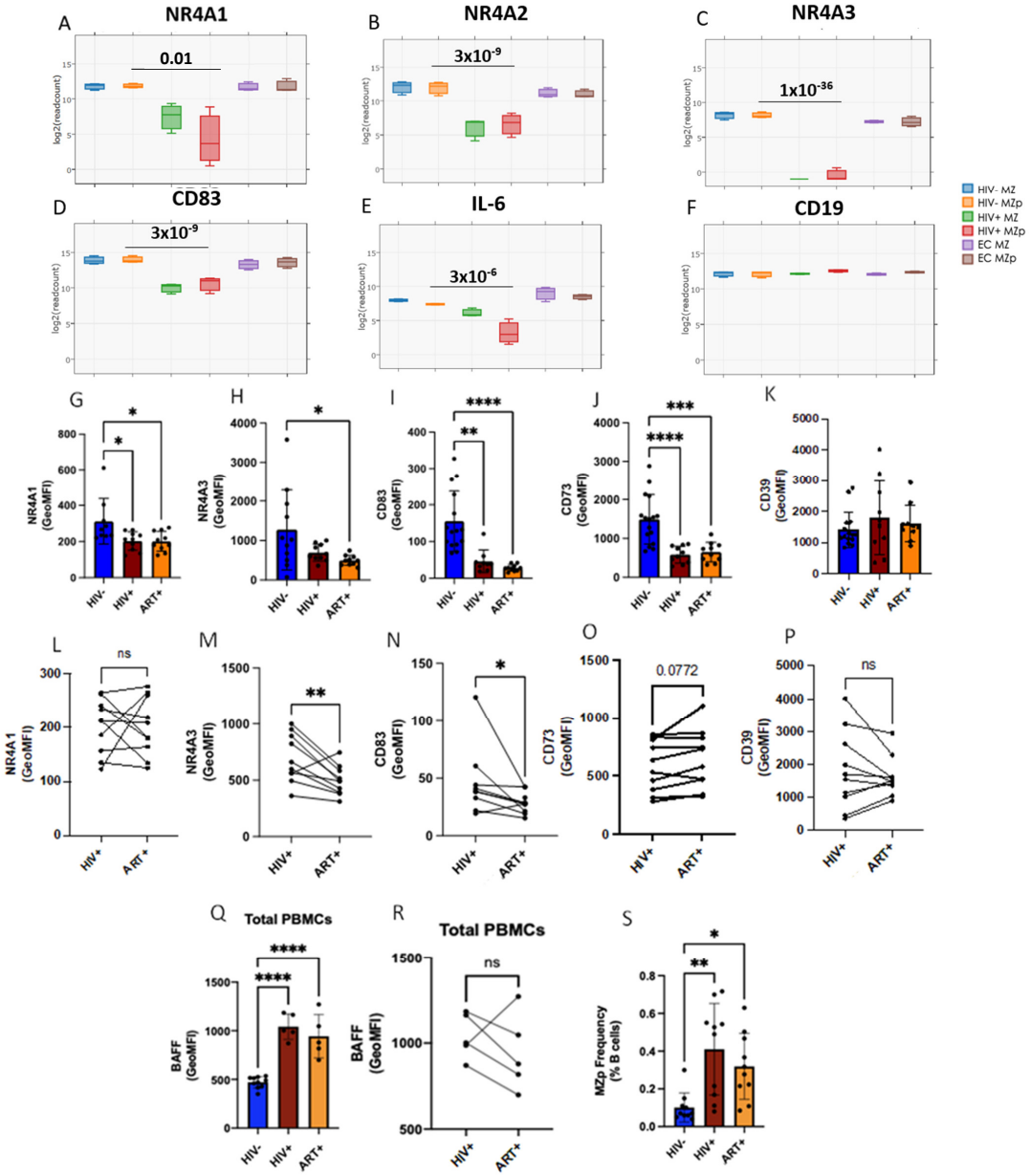

Figure 2. The expression levels of the Breg markers NR4A1, NR4A2 and NR4A3 are significantly downregulated in precursor-like marginal zone (MZp) B-cells from the blood of progressors. RNAseq analyses of MZ precursor-like (MZp) from the blood of controls (HIV−), 5–8 months progressors (HIV+) and elite controllers (EC) demonstrating gene expression levels of NR4A1 (**A**), NR4A2 (**B**), NR4A3 (**C**), CD83 (**D**), IL-6 (**E**) and CD19 (**F**), the latter which was used as a baseline strongly expressed B-cell gene (n =3 for each study group). Multicolor Flow-Cytometry analyses of protein expression levels of the Breg markers NR4A1, NR4A3, CD83, CD39 and CD73 were assessed on blood MZp B-cells, gated from total PBMCs of 15 controls and 10 progressors before and after ART. Shown are NR4A1 (**G**), NR4A3 (**H**), CD83 (**I**), CD73 (**J**) and CD39 (**K**) expression levels. Comparison between NR4A1 (**L**), NR4A3 (**M**), CD83 (**N**), CD39 (**O**) and CD73 (**P**) expression levels between primary infection and following ART for the same donors. Membrane BAFF expression levels were assessed on total PBMCs of 10 controls and 5 progressors before and after ART (**Q**). Comparison between membrane BAFF expression levels on total PBMCs of progressors before and after ART for the same donors (**R**). Relative frequencies of MZp in the blood of 10 controls and 10 progressors before and after ART (**S**). Protein expression levels were assessed by Geometric Mean of Fluorescence Intensity (GeoMFI). * $p < 0.05$; ** $p < 0.01$; *** $p < 0.001$; **** $p < 0.0001$. The Wald Test with Benjamini–Hochberg correction was used for RNAseq analysis (**A**–**F**). Normality was assessed with the Shapiro–Wilk test.

A One-Way ANOVA with a Tukey post-hoc test was used for testing statistical differences between groups in (**I**,**J**). A Kruskal–Wallis nonparametric test with Dunn's post-hoc test was used to assess statistical differences between groups in (**G**,**H**,**K**,**Q**,**S**). A paired *t*-test was used in assessing differences between individuals before and after ART in (**L**–**P**,**R**).

2.4. The Breg Function of Blood MZp B-Cells from Progressors Is Altered, despite ART

Given the important downregulation of Breg markers by blood MZp B-cells from progressors, and despite ART, we next sought to investigate whether the Breg function of MZp B-cells is altered in these individuals. In order to offset the low cellular yields of MZp B-cells in blood, High-Content Screening (HCS) by fluorescence in a confocal mode was used to assess the Breg function of sorted MZp B-cells on activated autologous $CD4^+$ T-cells (Figure 3A–D). We observed for controls that, while cell count, as determined by the amount of positive $CD4^+$ cells in each analyzed well (indicator of proliferation), seemed to be the same when $CD4^+$ T-cells were cultured alone or co-cultured with either MZp or $CD1c^-$ B-cells (negative control) (Figure 3E), mortality rates of $CD4^+$ T-cells were strikingly higher in the MZp: T-cell co-culture, suggesting regulation by controlled cell death (Figure 3F). As such, induction of apoptosis is a common regulatory function and has been described for Tregs [25]. Accordingly, we found that MZp B-cells strongly express CD274 (PD-L1, B7H1) when compared to other B-cell subtypes (Supplementary Figure S3). Furthermore, the addition of an anti-PD-1 blocking antibody to the MZp:T-cell co-culture diminished the mortality rates of $CD4^+$ T-cells, thus, supporting a role for the PD-1 (PDCD1)/PD-L1 pathway in MZp Breg function (Figure 3H). However, when assessing the Breg function of blood MZp from progressors, our results rather suggest that there is a lower induction of $CD4^+$ T-cell mortality in presence of MZp, and, strikingly, despite ART (Figure 3G). Altogether, our data suggest that HIV infection affects the Breg function of blood MZp B-cells, and this is not restored by ART.

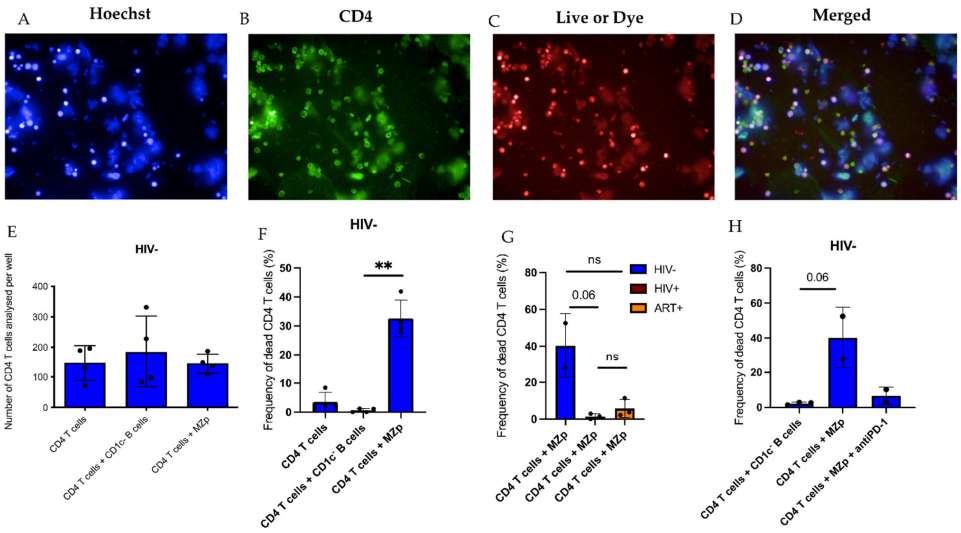

Figure 3. Impaired Breg function of blood precursor-like marginal zone (MZp) B-cells from progressors is not restored by ART. Breg function of MZp, as assessed by High-Content Screening (HCS). Shown are cell staining by Hoersch (**A**), $CD4^+$ T-cells staining by FITC (**B**), Live or Dye viability stain (**C**) and merged stains (**D**). $CD4^+$ T-cell count on each analyzed well (**E**). $CD4^+$ T-cells mortality following culture with Medium Alone or when co-cultured (3:1 ratio) with CD1c- B-cells (negative control) or MZp (**F**). $CD4^+$ T-cells mortality when co-cultured (3:1 ratio) with MZp B-cells from controls and progressors (with and without ART) (n =3) (**G**). $CD4^+$ T-cells mortality when co-cultured with MZp from controls with and without the addition of an anti-PD-1 blocking antibody at 2 µg/mL (**H**). Mortality was assessed as the relative frequency of Live or Dye cells when compared to the total $CD4^+$ T-cells. ** $p < 0.01$. Statistical differences between groups were assessed with the Kruskal–Wallis test with post-hoc Dunn test. Normality was assessed with the Shapiro–Wilk test.

2.5. Excess BAFF Directly Contributes to the Altered Breg Potential of MZp B-cells

Our RNA-seq analyses show that gene expression levels of BAFF-R are significantly downregulated by MZp from the blood of progressors compared to controls, while those of TACI and BCMA are not significantly affected (Supplementary Figure S4), albeit a trend for BCMA upregulation by blood MZp from progressors could be observed. These are consistent with our observations that expression levels of BAFF-R, but not those of TACI, are decreased on B-cells following culture with soluble BAFF (Supplementary Figure S5). To assess the relative contribution of excess BAFF on the dysregulation of MZp Breg capacities, blood MZp B-cells from controls have been sorted and cultured in the presence or absence of soluble BAFF at 50 ng/mL or 500 ng/mL overnight. Cells were then harvested for RNA extraction and a one-step qPCR for NR4A1, NR4A3 and CD83 mRNA quantification was performed, with GAPDH as a housekeeping gene. Our data show that at high concentrations (500 ng/mL), BAFF-treated blood MZp B-cells express lower NR4A1, NR4A3 and CD83 mRNA levels compared to unstimulated MZp B-cells, similar to that of sorted MZp B-cells from the blood of progressors (Figure 4A–C). Likewise, we enriched total B-cells from the tonsils of control donors and cultured them overnight with soluble BAFF at increasing concentrations. We found that tonsillar MZp B-cells treated with high BAFF concentrations show lower expression levels of NR4A1 and CD83 proteins compared to those treated with lower BAFF concentrations or medium alone (Figure 4D–G). Interestingly, we found that, as soluble BAFF concentrations increase, IL-10 expression levels decrease (Figure 4H,I). Of note, we had previously shown that IL-10 is highly expressed by ex vivo unstimulated blood MZp B-cells when compared to other B-cell populations ([26], and Supplementary Figure S6). Upon performing experiments with enriched tonsillar B-cells from control donors, we observed that the total tonsillar cells from different donors expressed varying levels of total membrane BAFF (Figure 4L). This difference was mainly attributable to DC-like (HLA-DR$^+$CD11c$^+$CD14$^-$CD3$^-$CD19$^-$) and MoDC-like (HLA-DR$^+$CD11c$^+$CD14$^+$CD3$^-$CD19$^-$) populations, as membrane BAFF expression on T-cells was similar between the donors (Figure 4M–O). Strikingly, tonsils expressing higher total membrane BAFF levels have reduced MZp Breg function, while tonsils expressing lower BAFF levels have an MZp Breg function comparable to that expected at a 1:3 ratio [14] (Figure 4J–K). Interestingly, this latter Breg function is altered upon the addition of high levels of soluble BAFF (Figure 4P). To further investigate the impact of membrane BAFF levels on MZp Breg capacities, blood-derived MoDC stimulated with LPS prior to paraformaldehyde fixation (Supplementary Figure S7) were co-cultured overnight with autologous blood B-cells at a 1:10 ratio. Blood MZp B-cells expression of regulatory markers were then assessed by flow cytometry (Supplementary Figure S7). We observe a trend for the downregulation of NR4A1 and NR4A3 expression levels by these blood MZp B-cells. Although this finding will need further investigation, it is tempting to speculate that DC-like and MoDC-like populations in secondary lymphoid tissues, which are known to interact with B-cell populations such as MZ B-cells [11], may influence MZp Breg activity through membrane and/or released BAFF expression levels.

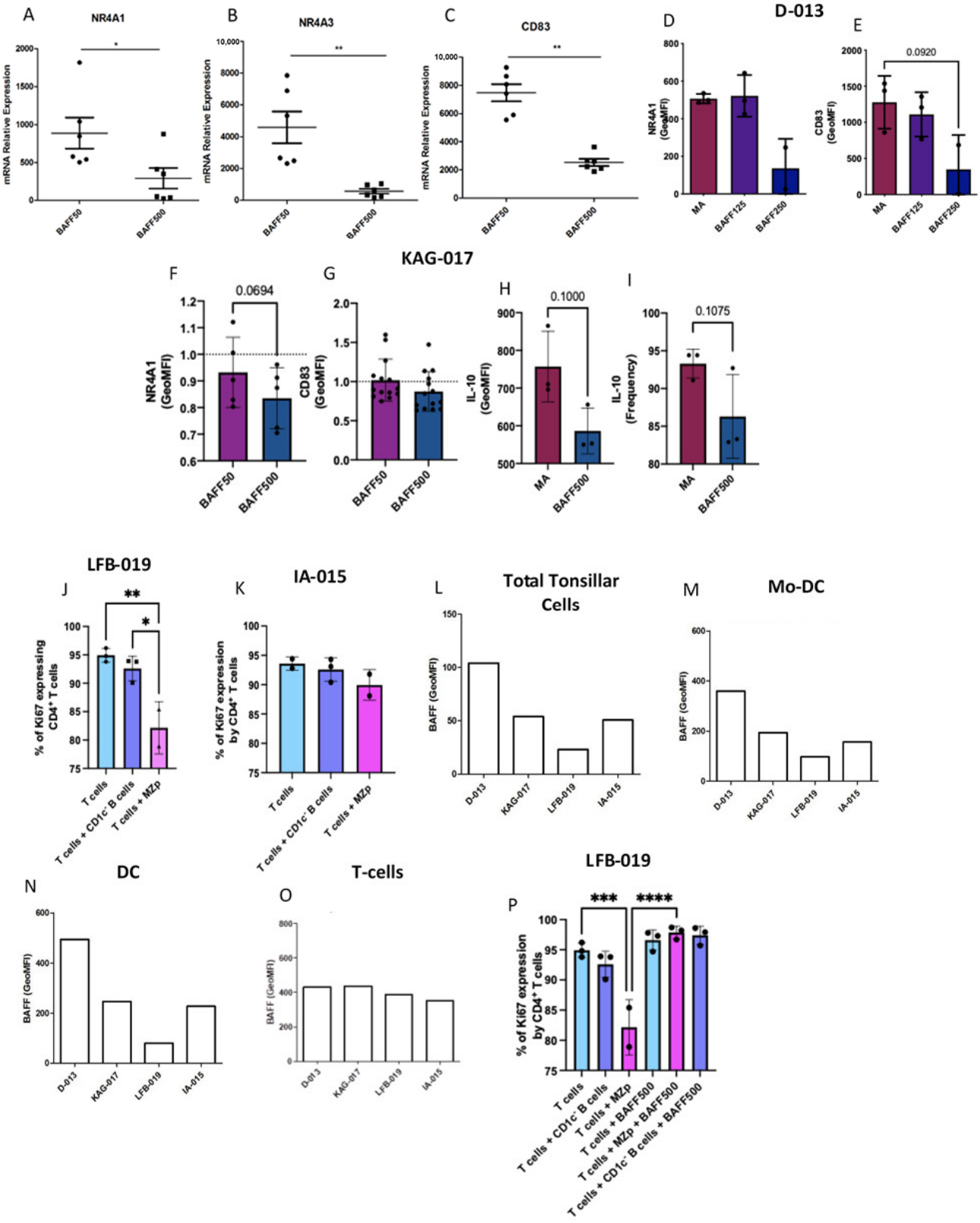

Figure 4. High levels of BAFF significantly downregulate precursor-like marginal zone (MZp) B-cell expression levels of immunoregulatory markers and influence their Breg function. qPCR analyses of NR4A1 (**A**), NR4A3 (**B**) and CD83 (**C**) mRNA relative expression levels by blood MZp B-cells from controls when cultured with 500 ng/mL soluble BAFF (2 donors, n = 3 each). Flow-cytometry analyses of BAFF-treated tonsillar B-cells from control donor D-013 (n=3) showing NR4A1 (**D**) and CD83 (**E**) protein expression levels. Flow cytometry analyses of BAFF-treated tonsillar B-cells from

control donor KAG-017 (n = 5) showing NR4A1 (**F**), CD83 (**G**) and IL-10 (**H**) expression levels as well as total relative frequencies of MZp expressing IL-10 (**I**). Data of (**F**) and (**G**) are shown as fold-over Medium Alone (MA) due to variabilities between different tonsillar samples from the same donor. Breg function of MZp B-cells from two different tonsillar donors, LFB-019 (**J**) and IA-015 (**K**) have been assessed as relative frequencies of $CD4^+$ T-cells expressing intracellular Ki67, as an indication of cell cycle entry. Flow-cytometry analyses of membrane BAFF levels from total tonsillar cells (**L**), Mo-DC (**M**), DC (**N**) and $CD3^+$ T-cells (**O**) from different tonsillar donors. Breg function of MZp B-cells from LFB-019 donor after treatment with high soluble BAFF (500 ng/mL) for 18 h, assessed as relative frequencies of $CD4^+$ T-cells expressing intracellular Ki67 (**P**). Relative frequencies of MZp expressing IL-10 were assessed relative to the percentage of total MZp B-cells. Relative frequencies of $CD4^+$ T-cells expressing Ki67 were assessed relative to the percentage of total $CD4^+$ T-cells. Expression levels were assessed with Geometric Mean of Fluorescence Intensity (GeoMFI). * $p < 0.05$; ** $p < 0.01$; *** $p < 0.001$; **** $p < 0.0001$; MA—Medium Alone; BAFF50—BAFF at 50 ng/mL; BAFF500—BAFF at 500 ng/mL. Statistical differences between groups were assessed with the Kruskal–Wallis test with post-hoc Dunn test. Normality was assessed with the Shapiro–Wilk test.

3. Discussion

There is a limitation of our study in the number of participants, and we believe adding further subjects in the future will strengthen the interpretation of our data. Nevertheless, the present study sheds some light on a better understanding of the important Breg potential of MZp B-cells, and its dysregulation in the context of chronic inflammation involving excess BAFF, such as is encountered in HIV infection. Importantly, MZp Breg potential was not restored by therapy. Several factors can be nourishing chronic inflammation and impacted immunocompetence. For example, we have shown that factors such as Nef persist in blood populations and directly contribute to BAFF over-expression, as do factors of microbial translocation, such as LPS [6]. These observations further stress the importance of very early treatment in cases of PHI to avoid the establishment of a chronic inflammatory status and its impact on immunocompetence [5].

We have previously shown that excess BAFF in the blood of progressors was concomitant with the dysregulation of the blood B-cell compartment, notably with increased frequencies of MZp B-cells [3], despite ART. In this study, we report that blood MZ populations, especially MZp B-cells from progressors, present a different transcriptomic profile compared to that of ECs and controls, suggestive of their being highly solicited and functionally impaired, with signs of exhaustion. Importantly, differences include the significant downregulation of gene transcripts for the molecules NR4A1, NR4A2, NR4A3 and CD83, which we have previously associated with the Breg potential of MZp B-cells in controls [15]. Furthermore, the protein expression levels of these molecules as well as those of CD73, also associated with regulatory capacities [27], are downregulated in blood MZp B-cells of progressors, despite ART. Even more importantly, we found that the Breg function of blood MZp B-cells is impaired in progressors and ART-treated individuals. Consistent with our previous observations [3], levels of BAFF were found to be in excess in the blood of progressors and ART-treated individuals selected for this study when compared to controls. Importantly, in vitro studies show that high levels of BAFF impact the expression of regulatory proteins by MZp B-cells from the tonsils of control donors and have a direct effect on their Breg function.

Our findings are suggesting that, in the context of HIV, which we characterize as a persistent excessive BAFF environment, MZ populations may be highly solicited, selected and expanded to produce antibodies at the expense of their Breg competence. As such, BAFF levels may dictate MZ B-cell activities, from Breg to antibody production, which in the context of HIV may be expedited, bypassing the Breg capacity, for tentative eradicative purposes. As to whether MZ B-cells antibody responses are beneficial or a nuisance to the host in the context of HIV remains to be established. As such, given the facts that HIV-Transgenic and BAFF-Transgenic mice presented a breakage of tolerance and autoimmunity [8,28–30], and that excess BAFF and MZ B-cell dysregulations have also been

reported in the context of autoimmune diseases such as Systemic Lupus Erythematosus (SLE) and Sjögren Syndrome (SS) [31], it would be sound to bear in mind that MZ B-cell antibody responses in the context of excess BAFF may be nourishing polyclonal, possibly auto-reactive, low-affinity antibody responses, whose pertinence in the battle against HIV have yet to be determined.

Notably, individuals with SLE or SS present a strong IFN signature, which promotes BAFF expression, reminiscent of what was observed in the context of chronic infections such as with HIV [32,33]. Thus, unsurprisingly, we found that genes that are associated with pro-inflammatory outcomes and ISG are upregulated in blood MZp B-cells of progressors. As such, we found that transcripts for genes involved in the regulation of IFN responsiveness such as OAS1, SP110 and IRF7 are highly upregulated in MZp B-cells of progressors when compared to ECs or controls. These data suggest that MZp B-cells are in a hyperactive state in the context of HIV, in a similar manner to that observed in autoimmune diseases such as SLE or SS.

Our GSEA analyses show that the major PI3K-AKT-MTOR pathway is downregulated in blood MZp B-cells from progressors. Mechanistic target of rapamycin kinase (MTOR) has been shown to be important for normal MZ B-cell function, as TACI signaling converges towards MTOR in order to lower the MZ activation threshold [34], which is in accordance with their role as first-line innate-like cells that respond quickly to blood-borne pathogens [12]. Interestingly, the transcript for the gene coding for BAFF-R is significantly downregulated by blood MZp B-cells of progressors, while the transcript for TACI remains highly expressed (Supplementary Figure S4). Unfortunately, we did not assess BAFF-R nor TACI protein expression levels by blood MZp in these individuals, but they are also likely to be modulated as we found that excess soluble BAFF in vitro downregulates cell surface expression levels of BAFF-R but not those of TACI on blood MZp (Supplementary Figure S5). It is therefore possible that, in progressors, reduced MZp expression of BAFF-R reflect ongoing exposure to increased amounts of its cognate ligand BAFF. Moreover, our data also suggest that BAFF signals may be mostly mediated via TACI during HIV infection. Importantly, the binding of BAFF to TACI allows the recruitment of TRAFs such as TRAF3 [35], which has been shown to inhibit the CREB pathway in B-cells [36], known to induce the expression of the NR4As [37,38], and which we find is also downregulated in MZp B-cells from progressors. Of note, a trend of low TRAF6 gene transcripts was found in progressors (p = 0.1), but not TRAF3 (Supplementary Figure S4), which could mean that TRAF3 could see a higher recruitment rate due to lower competition for TACI signals. These data suggest that the excess BAFF found during HIV infection may lead to CREB and NR4As downregulation via excess TACI signaling, and, thus, excess TRAF3 recruitment. Given the importance of CREB and NR4As in controlling cell activation [39], it is possible that their downregulation allows for MZp B-cells to maintain a hyperactive state despite MTOR downregulation. The fact that gene expression levels of BCMA show a trend for upregulation by blood MZp from progressors when compared to controls, could suggest differentiation towards an early plasmablast stage, as they also significantly upregulated CD38 gene transcripts (Supplementary Figure S4L).

Importantly, NR4A1, NR4A2 and NR4A3 gene transcripts were downregulated in a highly significant manner in MZp B-cells from the blood of progressors, with p values reaching orders of magnitude of 0.01, 10^{-9} and 10^{-36}, respectively. In addition, other important regulatory molecules that are directly modulated by NR4As such as CD83 and IL-6 [18] were also significantly downregulated. Consistently, blood MZp B-cells from progressors presented significantly lower protein expression levels of NR4A1, NR4A3 and CD83, and this was not restored by ART. The importance of NR4A transcription factors in immune regulation has been highlighted by the fact that NR4A1-3 double-knockout mice develop systemic autoimmune diseases [40]. Furthermore, in humans, downregulation of NR4As has been observed in the context of autoimmunity [40] and acute myeloid leukemia [41] whereby synthetic regulation of NR4A expression is currently used for eliminating cancerous cells [42]. Additionally, since the expression of NR4As

is necessary for the maintenance of FOXP3 expression by Tregs [17], there have been reports of several studies where those genes are targeted to modulate Treg responses in cancer [42]. Moreover, increasing NR4A1 expression in myeloid cells led to a diminished T-cell activation profile [21]. It is, thus, reasonable to think that NR4A modulation could be envisaged in view of restoring MZp Breg capacities, possibly in conjunction with therapies reducing excessive BAFF levels, already FDA-approved in the treatment of SLE.

We found similar observations for the ectonucleotidase CD73, the limiting molecule of the 2-aminoethanethiol dioxygenase (ADO) pathway [43]. Others have reported that the diminution of $CD73^+$ B-cells and $CD39^+CD73^+$ B-cells and the diminution of ADO correlated with a loss of $CD4^+$ T-cells and disease progression during HIV infection [44,45]. Interestingly, the HIV context is also associated with downregulated CD39 and CD73 expression levels in Tregs, despite ART [46]. In other chronic infections, such as hepatitis, a loss of CD73 and CD39 has also been observed and associated with viral load and high levels of inflammation [47]. It is also important to remember that ADO has been found to modulate NR4As expression levels via purinergic receptors such as $A2_A$ [48]. Therefore, the loss of CD39 and CD73 can contribute to a reduction of extracellular ATP conversion into ADO, which could promote a pro-inflammatory environment caused by the accumulation of extracellular ATP and a decrease in NR4A expression due to a decrease in the interaction between ADO and its receptors. Since the MTOR pathway is upregulated by the binding of ADO to its receptors [49], it is possible that the lower levels of ADO production by regulatory cell populations (MZp B-cells and others) contribute to the downregulation observed for the MTOR pathway.

Interestingly, we noticed that gene transcripts for Breg markers, such as IL-10 and the IL-10 regulatory transcription factor aryl hydrocarbon receptor (AHR), recently shown to be an important Breg marker in mice [50], were not affected in blood MZp from progressors, whereas others, such as transcription factor basic helix-loop-helix family member E40 (BHLHE40), also involved in IL-10 regulation, were significantly diminished when compared to controls (Supplementary Figure S4).

Consistent with their loss of several Breg markers, we show that blood MZp B-cells from progressors and ART-treated individuals lose their Breg function. We have previously shown that MZp B-cells from controls can control $CD4^+$ T-cell proliferation and that this involves signals delivered via CD83 [15]. Here, we show that the control of MZp B-cells on the activation of autologous $CD4^+$ T-cells may also involve controlled cell death and PD-1/PD-L1 signaling. Accordingly, the reduced Breg function observed for blood MZp from progressors, without and with ART, is concomitant with their lowered expression levels of PD-L1 (Supplementary Figure S3). Of note, the differences observed between PD-L1 gene transcripts, the expression levels of which were not affected in blood MZp from progressors, and PD-L1 protein expression levels, which were decreased, suggests that protein expression of PD-L1 could be affected by post-transcriptional mechanisms. Further studies are, thus, needed to confirm the relative involvement of all markers engaged in the MZp Breg function. Importantly, we show that excess BAFF can directly impact on MZp Breg capacities. Indeed, gene and protein expression levels of the regulatory markers NR4A1, NR4A3 and CD83 were downregulated in the presence of high-soluble and membrane BAFF levels, which also had an impact on IL-10 production, which could contribute further to the loss of Breg function in these cells.

When performing in vitro studies with tonsils from control donors, we noticed that BAFF levels varied between donors and this influenced in vitro MZp Breg capacities. Variations of BAFF levels between each donor appear to be especially attributable to levels expressed by myeloid cells such as DC-like and MoDC-like populations. As such, DC are an important source of BAFF, and have been shown to interact with B-cells in T-independent manners [12], and could have, thus, modulated the tonsillar MZ B-cell environment. Of note, in HIV-Tg mice, we have observed that myeloid DCs accumulated in the expanded MZ of these mice [51]. We have previously published that HIV infection increases BAFF levels on DC and MoDCs via Nef [7]. Likewise, elements of microbial translocation, such

as LPS were also shown to increase BAFF expression by MoDCs ([7], Supplementary Figure S7). Our findings point to BAFF as being a major contributor to the loss of MZp Breg capacities during HIV infection. Similar to that observed for SLE and other rheumatic disorders, there is growing evidence that BAFF is in excess in contexts of cancer, and could also play a role in the pathogenesis of several inflammatory chronicity, such as multiple sclerosis and HBV infection [32], suggesting that excess BAFF and dysregulated MZp may be important indicators of deterioration of immunocompetence.

We found relatively higher gene expression levels of exhaustion markers, such as FCRL5 and CD85j, and negative regulators, such as CD22 and CD72, in blood MZp B-cells of progressors when compared to controls, which suggests a higher activation index. Additionally, MZp B-cells express both IL-21R and TLR7 (Supplementary Figure S4), which signals are important to drive B-cell differentiation towards an "age associated"-like exhausted B-cell profile. As such, blood MZp B-cells from progressors also possess higher gene expression levels of T-bet and CD11c, a characteristic related to age-associated B-cells, and shared by a similar heterogeneous population found to be expanded in autoimmunity, chronic infections, antibody-mediated rejection in organ transplants [52–54] and critically ill patients with SARS-CoV-2 [55]. Interestingly, B-cells that express T-bet and CD11c have been associated with their accumulation at extra-follicular sites and the production of immunoglobulins (IG) of poor affinity [56].

To date, many groups have identified MZ-like populations with Breg capacities vs. T-cells, in non-cognate fashions, in vitro, in murine models and humans (recently reviewed by [57]). Herein, our data suggest that such Breg capacity of MZp is greatly reduced in progressors, and not restored by ART, and this possibly involves the excessive BAFF levels reported for these individuals. As to whether MZp can exert their Breg functions through cognate interactions with CD4+ T-cells, needs further experimentation and is beyond the scope of our study but deserves to be addressed. Mouse MZ B-cell populations have been shown to migrate to T-cell zones of secondary lymphoid organs (SLO), and activate CD4+ T-cells in a HEL-dependent manner [58]. This, and the fact that MZ B-cell populations have the capacity to shuttle to follicular areas [59], and that MZ B-cells were shown to possess an atheroprotective role attributed to their NR4A1 expression [23,24], all point to the capacity of MZ populations to be recruited to outer MZ areas of SLO, in given situations. Furthermore, MZ B-cells are able to present lipidic antigens to invariant natural killer T-cells (iNKT), in the context of CD1, which confer activation via, notably, the CD40–CD40 ligand (CD40L) pathway [60]. All of which support their influence on several cell types. The capacity of MZ B-cell populations to perform antigen presentation and Breg activity, or to differentiate towards Ig production, may be dictated by the overall situation and environment (reviewed in [61]).

4. Materials and Methods

4.1. Specimen Collection and Clinical Data

Cryopreserved blood specimens from 13 male HIV-1-infected classic progressors were selected from the Montreal PHI cohort specimen bank. For simplicity, the term "HIV" is used throughout this manuscript. Clinical data from these individuals can be found in Table 1. The date of infection was estimated based on clinical and laboratory results, using criteria established by the Acute HIV Infection and Early Disease Research Program (National Institute of Allergy and Infectious Diseases [NIAID], Bethesda, MD). Blood samples had been collected at two time points: the acute phase of infection (i.e., 0–3 months after HIV acquisition) and/or early phase of infection (i.e., 5–8 months after HIV acquisition), as well as 96 weeks after HIV acquisition, with an average of 92 weeks of ART treatment (Table 1). Cryopreserved blood samples from three male EC were obtained from the Montreal Long Term Non-Progressor (LTNP) cohort [26]. Cryopreserved blood samples from 18 male HIV-negative healthy volunteers were obtained from the Montreal PHI cohort, to be used as controls. Plasma viral loads and blood CD4+ T-cell counts were determined as reported previously [62]. None of the subjects had syphilis, hepatitis B, or hepatitis C.

Written informed consent was obtained from all subjects, and the research conformed to the guidelines of, and was approved by, the University of Montreal Hospital Research Center Ethics Review Board (project reference SL05.028).

4.2. Cell Sorting of Human Blood MZ and MZp B-Cells, RNA Isolation and Sequencing

Peripheral blood mononuclear cells (PBMCs) from 3 controls, 3 HIV-classic progressors at 5–8 months post-infection and 3 ECs had been isolated on Ficoll gradients, re-suspended in cryopreservation medium containing 90% heat-inactivated fetal bovine serum (hi-FBS) (Wisent Inc., Montreal, QC, Canada) and 10% dimethyl sulfoxide (DMSO), and stored in liquid nitrogen until use. Cells were thawed, washed in IMDM (Iscove's Modified Dulbecco's Medium, Gibco Life Technologies, New York, NY, USA), and processed for cell sorting with a FACSAriaIII apparatus. Live/dead exclusion was performed using LIVE/DEAD Fixable Aqua Dead Cell Stain (Invitrogen Thermo Fisher Scientific, Eugene, OR, USA). Non-specific binding sites were blocked using fluorescence-activated cell sorting (FACS) buffer (1× PBS, 2% hi-FBS) supplemented with 20% hi-FBS and 10 µg mouse IgG (Sigma-Aldrich, St-Louis, MO, USA). Cells were stained using the following conjugated mouse anti-human monoclonal antibodies (mAbs): PacificBlue-anti-CD19, APC-Cy7-anti-CD10 (BioLegend, San Diego, CA, USA), AlexaFluor700-anti-CD27, FITC-anti-IgM, PE-anti-CD21 (BD-Biosciences, San Jose, CA, USA), PerCP-eFluor710-anti-CD1c (eBioscience, San Diego, CA, USA). Sorted live $CD19^+CD1c^+IgM^+CD27^+CD21^{hi}CD10^-$ mature MZ and $CD19^+CD1c^+IgM^+CD27^+CD21^{lo}CD10^+$ MZp B-cells were >95% pure. Total RNA was extracted using RNeasy Micro Kit (Qiagen) according to the manufacturer's instructions. RNA integrity was validated using an RNA Pico Chip on the Agilent BioAnalyzer 2100, and RNA was sent to the IRIC Genomics Core Facility for RNA-seq transcriptomic profiling and analysis. Libraries were prepared using Clontech Ultra Low RNA SMARTer v4 (Takara) and sequenced on a HiSeq2000. Genes with false discovery rate (FDR) values < 0.05 were considered to be differentially expressed. Gene expression levels were compared using raw read counts and the negative binomial distribution model implemented in DESEq2 [63], a differential expression analysis package developed for R, which adjusts for sample variations with the assumption that the vast majority of genes should have correlating expression levels. More specifically, the regularized log transformation (rlog) implemented in DESeq2 was used to transform raw data into log2 (readcount) for analysis and visualization.

4.3. Volcano Plot and Gene Set Enrichment Analyses (GSEAs)

The volcano plot was created using Python 3.9.5. First, a comma-separated value (CSV) file containing the raw RNA-Seq gene expression data was imported into a pandas 1.3.1 DataFrame. Each gene was assigned the color blue if significantly upregulated/downregulated ($p < 0.05$ and fold change > or <1), otherwise it was assigned the color gray. Annotations for the genes were assigned black if significantly upregulated/downregulated beyond the specified *p*-value and *n*-fold change. Otherwise, they were assigned red labels regardless of their *p*-values or *n*-fold-changes if they appear in a specified list of genes to highlight. Finally, the volcano plot was generated using Matplotlib 3.4.2. Specified *p*-values and *n*-fold lines were drawn as blue lines. The total number of upregulated/downregulated genes were displayed in the upper right/left corners, respectively.

Gene Set Enrichment Analyses (GSEAs) were produced using the software application GSEA 4.1.0, developed by the Broad Institute, as previously published [64,65]. Required input files are the expression data, the phenotype labels, and the gene set. The expression data file consists of a table whose first column is gene name, followed by gene description, followed by the genes' expression values for each sample. The phenotype labels file associates a phenotype label (e.g., HIV+ or HIV−) with each sample in the group. Gene sets for this manuscript were downloaded from the Broad Institute's Molecular Signatures Database (MSigDB) v.7.4.; they are KEGG's MTOR pathway (KEGG_MTOR_SIGNALING_PATHWAY) and Transcription Factors' CREB/cJUN pathway

(CREBP1CJUN_01) The software generates an analysis for each gene set containing the Net Enrichment Score (NES), false discovery ratio (q-value) and p-value. A gene set is considered significantly modulated if q-value and p-value <0.05.

4.4. Multicolor Flow-Cytometry

PBMCs from 15 controls and 10 progressors (without and with ART) were processed for flow cytometry as previously described [15]. Briefly, live/dead exclusion was performed using Aqua-LIVE/DEAD Fixable Stain (Invitrogen Life technologies, Eugene, OR, USA). Non-specific binding sites were blocked using FACS buffer (1 × PBS, 2% hi-FBS, and 0.1% sodium azide) supplemented with 20% hi-FBS, 10 µg mouse IgG (Sigma-Aldrich, St-Louis, MO, USA) and 5 µg Human BD FCBlock (BD Biosciences, Franklin Lakes, NJ, USA). The following mouse anti-human conjugated mAbs were used to detect extracellular markers on B-cells: APC Anti-CD19, BB515 Anti-IgM, BV421 Anti-CD10, BUV395 Anti-CD73, BV786 Anti-CD39, PE-Cy7 Anti-CD83 (BD Biosciences, Franklin Lakes, NJ, USA) and PerCP-eFluor 710 Anti-CD1c (eBioscience, San Diego, CA, USA). For means of verifying MZ and MZp B-cell populations as to CD21 expression levels, we had three different staining cocktails, each identical except for having a variation for the PE slot, i.e., (1) PE-anti-NR4A1, (2) PE-anti-NR4A3, and (3) PE-anti-CD21, to verify that the MZp were indeed CD21lo when compared to MZ. For detection of membrane BAFF expression levels, the mouse anti-human PE Anti-BAFF (clone 1D6, Invitrogen, Waltham, MA, USA) was used. For assays with Monocyte Derived-Dendritic Cells (MoDC) (see below), the following conjugated mouse anti-human mAbs were used: PE-Cy5.5 Anti-CD11c (Invitrogen, Waltham, MA, USA), PE-Cy7 Anti-HLA-DR and BV786 Anti-CD14 (BD Biosciences, Franklin Lakes, NJ, USA) Intra-nuclear labeling was performed using the FoxP3/Transcription Factor Staining Buffer Set (eBioscience, San Diego, CA, USA). Non-specific binding sites were blocked using 20% hi-FBS. The mAbs used were the PE-conjugated human REA clone anti-mouse NR4A1, the cross-reactivity of which with human has been previously assessed [15], and compared to the PE-conjugated human REA isotype control (Miltenyi Biotech, Bergisch Gladbach, Germany), as well as the PE-conjugated mouse anti-human NR4A3 (Santa Cruz Biotechnology, Dallas, TX, USA). Intra-cellular labeling for the detection of IL-10 was performed using the Intracellular Fixation & Permeabilization Buffer Set (eBioscience, San Diego, CA, USA) and the PE mouse anti-human Anti-IL-10 mAb (Biolegend, San Diego, CA, USA). Cells were kept at 4 °C in 1.25% paraformaldehyde until analysis. Data acquisition was performed with FACSFortessa (BD-Biosciences, Franklin Lakes, NJ, USA) for blood PBMC samples and LSRIIB (BD-Biosciences) for tonsillar samples (described below). Analyses were done with FlowJo 10 software and GraphPad Prism. All stainings were compared to that of fluorescence minus one (FMO) values and isotype controls (see gating strategy in Supplementary Figure S1). Anti-mouse Ig(κ) Compbeads and CS & T Beads were used to optimize fluorescence compensation settings and calibrate the LSRIIB, respectively.

4.5. Human Tonsillar B-Cells

Human tonsils from controls, who had undergone surgical tonsillectomy, were mechanically processed and cells were cryopreserved in liquid nitrogen until use, as described above. Cells were thawed and washed in IMDM, and B-cells were negatively enriched >95% by an immunomagnetic-based technology (Dynabeads Untouched Invitrogen Life technologies). Total B-cells were subsequently cultured at a concentration of 10^6 cells/mL in IMDM supplemented with 10^{-4} β-2-mercaptoethanol, 10% hi-FBS, and 1% penicillin/streptomycin, in the absence or presence of stimuli (PMA/ionomycin or human recombinant soluble BAFF/BLyS/TNFSF13B Protein (R & D System)) for 18 h at 37 °C and 5% CO_2. Cells were cultured with Brefeldin A for the last 4 h of incubation prior to staining for intra-cellular IL-10 expression levels. Cells were recovered and processed for flow-cytometry as stated above.

4.6. qPCR Characterisation of NR4A1, NR4A3 and CD83 mRNA Expression Levels by Blood MZp B-Cells

MZp B-cells sorted from the blood of controls, and cultured with or without soluble BAFF at 50 ng/mL or 500 ng/mL overnight, were assessed for their expression levels of NR4A1, NR4A3, and CD83 mRNA by qPCR. Briefly, blood MZp B-cells were cell-sorted as stated above and lysed with TRIzol solution (ThermoFisher, Waltham, NJ, USA). mRNA was extracted with the phenol/chloroform technique. The quality of extracted mRNA (260/280 and 260/230 ratios) was assessed with a DS-11 FX Spectrophotometer (DeNovix, Wilmington, DE, USA). RNA was considered pure when the 260/280 ratio was above 1.8 and the 260/2360 ratio was above 2.0. One-step qPCR was done with the QuantiNova SYBR Green qPCR Kit (QIAGEN) by using 20 ng RNA from each donor. Glyceraldehyde-3-phosphate dehydrogenase (GAPDH) was used as a housekeeping gene. The primers used were: NR4A1 forward: 5′-CCAGCACTGCCAAACTGGACT A-3′; NR4A1 reverse: 5′-CTCAGCAAAGCCAGGGATCTTC-3′; NR4A3 forward: 5′-CCCTTTCAGACTATCTGTAC-GGAC-3′; NR4A3 reverse: 5′-CTCAGTGTTGGAATGGTAAAAGAAG-3′; CD83 forward: 5′-TCCTGAGCTGCGCCTACAG-3′; CD83 reverse: 5′-GCAGGGCAAGTCCACATCTT-3′; GAPDH forward: 5′-GTCTCCTCTGACTTCAACAGCG-3′; and GAPDH reverse: 5′-ACCACCCTGTTGCTGTAGCCAA-3′. Ct values were determined with the thermocycler Corbett Research RotorGene 6000. Ct is the value of the number of cycles necessary for the number of RNA copies to reach a precise fluorescence threshold. The relative expression of mRNAs was determined by the ΔCt method, where the Ct values of each gene are subtracted from the Ct value of the GAPDH housekeeping gene. mRNA expression = $(2^{-\Delta Ct}) \times 10{,}000$.

4.7. Breg Functional Assays

4.7.1. For Assays with Tonsillar Populations

As previously described [14], live autologous MZp B-cells, CD1c$^-$ B-cells (negative control) and CD4$^+$ T-cells were sorted (see description above for RNA-Seq) from human tonsillar samples of control donors. CD4$^+$ T-cells were cultured alone or co-cultured with either of the B-cell populations at a ratio of 3:1 for 36 h at 37 °C and 5% CO_2; on anti-CD3 (2 μg/mL) (ULTRA-LEAF Biolegend, San Diego, CA, USA)-coated flat-bottomed 96 well plates with soluble anti-CD28 (2 μg/mL) (ULTRA-LEAF Biolegend, San Diego, CA, USA); and with or without human recombinant soluble BAFF at 500 ng/mL. The read-out of the Breg function was based on cell cycle entry of CD4$^+$ T-cells, which was assessed by flow-cytometry analyses of intra-nuclear Ki67 expression levels using the PE-mouse anti-human Ki67 mAb (eBioscience, San Diego, CA, USA), as described above.

4.7.2. For Assays with Blood Cell Populations

Because of limited quantities of cells in our populations of interest, we proceeded to High-Content Screening (HCS) assays, the read-out for Breg function of which was based on the mortality of CD4$^+$ T-cells rather than cell cycle entry. As described above, autologous MZp B-cells, CD1c$^-$ B-cells (negative control) and CD4$^+$ T-cells were sorted (see description above for RNA-Seq) from human PBMCs of controls and progressors (without and with ART). CD4$^+$ T-cells were cultured alone or co-cultured with either of the B-cell populations at a ratio of 3:1 for 60 h at 37 °C and 5% CO_2 on anti-CD3 (2 μg/mL) (ULTRA-LEAF Biolegend, San Diego, CA, USA)-coated flat-bottomed 384 CellCarrier Ultra microplates (PerkinElmer, Waltham, MA, USA) with soluble anti-CD28 (2 μg/mL) (ULTRA-LEAF Biolegend, San Diego, CA, USA) in the presence or absence of a mouse anti-human PD1 (2 μg/mL) blocking antibody (Biolegend, San Diego, CA, USA). CD4$^+$ T-cells were identified using a mouse-anti-human CD4 (OKT4 clone) primary mAb and FITC goat anti-mouse secondary antibody (Invitrogen, Waltham, MA, USA). The cells were then fixed using 4% paraformaldehyde before the nuclei were stained with Hoescht 33342 (Invitrogen, Waltham, MA, USA). Data acquisition was performed with Operetta and analyses were done using Harmony and GraphPad Prism. The algorithm excluded debris based on Hoescht intensity, then excluded B-cells based on FITC negativity, and dead cells were

counted based on the intensity of Live or Dye CellMask signals of a mortality control. To this end, $CD4^+$ T-cells were cultured alone in a flat-bottomed 96-well plate for 60 h in the same conditions and then collected and placed at 56 °C in a water bath for 45 min. The cells were then stained with Live or Dye CellsMask for Live/Dead exclusion.

4.8. MoDC: B-Cell Co-Cultures

To assess the impact of membrane-bound BAFF on MZp expression levels of Breg markers, MoDC were generated from blood samples of controls, as previously described [7]. Briefly, cryopreserved PBMCs were thawed and washed in IMDM and $CD14^+$ monocytes were negatively enriched >95% by an immunomagnetic-based technology (Dynabeads Untouched Invitrogen Life technologies). Total $CD14^+$ monocytes were subsequently cultured at a concentration of 5×10^5 cells/mL in IMDM supplemented with 10^{-4} β-2-mercaptoethanol, 10% hi-FBS, 1% penicillin/streptomycin, 100 ng/mL Human Recombinant IL-4, and 250 ng/mL Human Recombinant GM-CSF (ThermoFisher, Waltham, NJ, USA) for six days at 37 °C and 5% CO_2. During the third day of incubation, 30% of growth conditions were reinstated. At day 6, MoDC purity was assessed by flow cytometry as stated above (>90% of cells were HLA-$DR^+CD11c^+CD14^{+/-}$). MoDC were subsequently cultured, with and without LPS (2 µg/mL), overnight at 37 °C and 5% CO_2. MoDC were then assessed for membrane BAFF expression levels by flow-cytometry as stated above, fixed in 0.25% paraformaldehyde, washed and co-cultured with autologous total B-cells (enriched as described above) at a 1:10 ratio overnight at 37 °C and 5% CO_2. Lastly, B-cells were harvested and processed for flow cytometry, as stated above.

4.9. Statistical Analyses

Statistical significance of differences between groups was assessed with a one-way ANOVA with post-hoc Tukey test for data normally distributed or otherwise with the Kruskal–Wallis test with post-hoc Dunn test. Statistical significance of difference in clinical data between progressors before and after ART was assessed with the Wilcoxon matched-pairs test. Statistical significance of difference between progressors and EC was assessed with the Mann–Whitney U test. Analyses were performed using GraphPad Prism 9.1.1, on Windows. Results were considered significant when $p < 0.05$.

5. Conclusions

Our observations are essential to help develop strategies viewed at restoring MZp immune surveillance activities. To this end, existing strategies, such as dihydroergotamine (DHE) viewed to upregulate NR4As expression levels could be envisaged to reinstate MZp Breg capacities. Additionally, BAFF-blocking therapies, such as Belimumab (Benlysta), which is FDA-approved in treating SLE, could be contemplated to try to control BAFF levels in order to lower the inflammatory burden and restore B-cell immune competence.

Supplementary Materials: The following supporting information can be downloaded at: https://www.mdpi.com/article/10.3390/ijms232315142/s1.

Author Contributions: K.D.-L., M.A., J.P. managed all the parameters regarding the study participants. J.C.-C. prepared the samples for RNA-sequencing (IRIC). K.D.-L. and M.A. performed the flow cytometry and Breg experiments. K.D.-L. performed Breg experiments by HCS. M.A. performed the qPCR, and MoDC experiments. M.B. did the first assays with soluble BAFF and tonsillar samples. K.D.-L., M.A., J.P., M.R. analyzed the data and wrote the article. M.P. and M.A. performed the Volcano plot and GSEA statistical analyses. K.D.-L. and M.A. produced graphs and layouts. J.P. and M.R. designed the concept. J.-P.R. and C.T. manage the Montreal LTNP and PHI cohorts, and provided all the blood samples. M.-C.Q., N.B. and D.E.K. managed and provided the human tonsillar samples. All authors have read and agreed to the published version of the manuscript.

Funding: This work was supported by grant # PJT-148529 to M.R. and J.P. from the Canadian Institutes of Health Research (CIHR) and by the Réseau SIDA from the Fonds de Recherche du Québec en Santé (FRQS). D.E.K. is a FRQS Merit Research Scholar.

Institutional Review Board Statement: The study was conducted in accordance with the Declaration of Helsinki, and the research conformed to the guidelines of, and was approved by, the University of Montreal Hospital Research Center Ethics Review Board (project reference SL05.028).

Informed Consent Statement: Written informed consent was obtained from all subjects involved in this study.

Acknowledgments: We are grateful to Mario Legault for the clinical data. We are grateful to Raphaële Lambert, Jennifer Huber and Patrick Gendron (IRIC Genomic and Bioinformatics core facilities) for RNASeq transcriptomic and data analyses, respectively. We are grateful to Guillaume Beaudoin-Bussières for the help with the BSL3 cell culture. We are also grateful to Erik Joly for his help during troubleshooting and for establishing the algorithm for the HCS experiments. We are grateful to Dre Dominique Gauchat, Philippe St-Onge and Gaël Dulude for their support with the CHUM cytometry platform. We are grateful to Audray Fortin and Elise Caron for their help in establishing the HCS protocol. We are grateful to Pavel Chrobak and Bertrand Allard for fruitful discussions. And lastly, we are grateful to the individuals who graciously donated the samples required for this study.

Conflicts of Interest: The authors declare that the research was conducted in the absence of any commercial or financial relationships that could be construed as a potential conflict of interest.

References

1. UNAIDS. Global HIV & AIDS Statistics—Fact Sheet. 2021. Available online: https://www.unaids.org/en/resources/fact-sheet (accessed on 8 November 2022).
2. De Pablo-Bernal, R.S.; Ruiz-Mateos, E.; Rosado, I.; Dominguez-Molina, B.; Alvarez-Ríos, A.I.; Carrillo-Vico, A.; De La Rosa, R.; Delgado, J.; Muñoz-Fernández, M.A.; Leal, M.; et al. TNF-α levels in HIV-infected patients after long-term suppressive cART persist as high as in elderly, HIV-uninfected subjects. *J. Antimicrob. Chemother.* **2014**, *69*, 3041–3046. [CrossRef]
3. Fontaine, J.; Chagnon-Choquet, J.; Valcke, H.S.; Poudrier, J.; Roger, M.; the Montreal Primary HIV Infection and Long-Term Non-Progressor Study Groups. High expression levels of B lymphocyte stimulator (BLyS) by dendritic cells correlate with HIV-related B-cell disease progression in humans. *Blood* **2011**, *117*, 145–155. [CrossRef]
4. Aranguren, M.K.D.-L.; El-Far, M.; Chartrand-Lefebvre, C.; Routy, J.-P.; Tremblay, C.; Durand, M.; Poudrier, J.; Roger, R. Subclinical Atherosclerosis is Associated with Discrepancies in BAFF and APRIL Levels and Altered Breg Potential of Precursor-like Marginal Zone B-cells in HIVTreated Individuals. *bioRxiv* **2022**. [CrossRef]
5. Moir, S.; Fauci, A.S. B cells in HIV infection and disease. *Nat. Rev. Immunol.* **2009**, *9*, 235–245. [CrossRef]
6. Poudrier, J.; Chagnon-Choquet, J.; Roger, M. Influence of Dendritic Cells on B-Cell Responses during HIV Infection. *Clin. Dev. Immunol.* **2012**, *2012*, 592187. [CrossRef]
7. Chagnon-Choquet, J.; Gauvin, J.; Roger, J.; Fontaine, J.; Poudrier, J.; Vassal, A.; Legault, M.; Routy, J.P.; Tremblay, C.; Thomas, R.; et al. HIV Nef Promotes Expression of B-Lymphocyte Stimulator by Blood Dendritic Cells During HIV Infection in Humans. *J. Infect. Dis.* **2014**, *211*, 1229–1240. [CrossRef]
8. Poudrier, J.; Weng, X.; Kay, D.G.; Paré, G.; Calvo, E.L.; Hanna, Z.; Kosco-Vilbois, M.H.; Jolicoeur, P. The AIDS Disease of CD4C/HIV Transgenic Mice Shows Impaired Germinal Centers and Autoantibodies and Develops in the Absence of IFN-γ and IL-6. *Immunity* **2001**, *15*, 173–185. [CrossRef]
9. Poudrier, J.; Soulas, C.; Chagnon-Choquet, J.; Burdo, T.; Autissier, P.; Oskar, K.; Williams, K.C.; Roger, M. High Expression Levels of BLyS/BAFF by Blood Dendritic Cells and Granulocytes Are Associated with B-cell dysregulation in SIV-Infected Rhesus Macaques. *PLoS ONE* **2015**, *10*, e0131513. [CrossRef]
10. Fourcade, L.; Sabourin-Poirier, C.; Perraud, V.; Faucher, M.-C.; Chagnon-Choquet, J.; Labbé, A.-C.; Alary, M.; Guédou, F.; Poudrier, J.; Roger, M. Natural Immunity to HIV is associated with Low BLyS/BAFF levels and low frequencies of innate marginal zone like CD1c+ B-cells in the genital tract. *PLoS Pathog.* **2019**, *15*, e1007840. [CrossRef]
11. Sabourin-Poirier, C.; Fourcade, L.; Chagnon-Choquet, J.; Labbé, A.C.; Alary, M.; Guédou, F.; Poudrier, J.; Roger, M. Blood B Lymphocyte Stimulator (BLyS)/BAFF levels may reflect natural immunity to HIV in highly exposed uninfected Beninese Commercial Sex Workers. *Sci. Rep.* **2016**, *6*, 32318. [CrossRef]
12. Cerutti, A.; Cols, M.; Puga, I. Marginal zone B cells: Virtues of innate-like antibody-producing lymphocytes. *Nat. Rev. Immunol.* **2013**, *13*, 118–132. [CrossRef] [PubMed]
13. He, B.; Qiao, X.; Klasse, P.J.; Chiu, A.; Chadburn, A.; Knowles, D.M.; Moore, J.P.; Cerutti, A. HIV-1 Envelope Triggers Polyclonal Ig Class Switch Recombination through a CD40-Independent Mechanism Involving BAFF and C-Type Lectin Receptors. *J. Immunol.* **2006**, *176*, 3931–3941. [CrossRef] [PubMed]
14. Henrick, B.M.; Yao, X.-D.; Zahoor, M.; Abimiku, A.; Osawe, S.; Rosenthal, K.L. TLR10 Senses HIV-1 Proteins and Significantly Enhances HIV-1 Infection. *Front. Immunol.* **2019**, *10*, 482. [CrossRef]
15. Doyon-Laliberté, K.; Chagnon-Choquet, J.; Byrns, M.; Aranguren, M.; Memmi, M.; Chrobak, P.; Stagg, J.; Poudrier, J.; Roger, M. NR4A Expression by Human Marginal Zone B-Cells. *Antibodies* **2019**, *8*, 50. [CrossRef]

16. Sekiya, T.; Kashiwagi, I.; Yoshida, R.; Fukaya, T.; Morita, R.; Kimura, A.; Ichinose, H.; Metzger, D.; Chambon, P.; Yoshimura, A. Nr4a receptors are essential for thymic regulatory T cell development and immune homeostasis. *Nat. Immunol.* **2013**, *14*, 230–237. [CrossRef]
17. Bandukwala, H.S.; Rao, A. 'Nurr'ishing Treg cells: Nr4a transcription factors control Foxp3 expression. *Nat. Immunol.* **2013**, *14*, 201–203. [CrossRef]
18. Duren, R.P.; Boudreaux, S.P.; Conneely, O.M. Genome Wide Mapping of NR4A Binding Reveals Cooperativity with ETS Factors to Promote Epigenetic Activation of Distal Enhancers in Acute Myeloid Leukemia Cells. *PLoS ONE* **2016**, *11*, e0150450. [CrossRef]
19. Ashouri, J.; Weiss, A. Endogenous Nur77 Is a Specific Indicator of Antigen Receptor Signaling in Human T and B Cells. *J. Immunol.* **2016**, *198*, 657–668. [CrossRef]
20. Odagiu, L.; May, J.; Boulet, S.; Baldwin, T.A.; Labrecque, N. Role of the Orphan Nuclear Receptor NR4A Family in T-Cell Biology. *Front. Endocrinol.* **2021**, *11*, 624122. [CrossRef]
21. Tel-Karthaus, N.; Kers-Rebel, E.D.; Looman, M.W.; Ichinose, H.; De Vries, C.J.; Ansems, M. Nuclear Receptor Nur77 Deficiency Alters Dendritic Cell Function. *Front. Immunol.* **2018**, *9*, 1797. [CrossRef]
22. Iizuka-Koga, M.; Nakatsukasa, H.; Ito, M.; Akanuma, T.; Lu, Q.; Yoshimura, A. Induction and maintenance of regulatory T cells by transcription factors and epigenetic modifications. *J. Autoimmun.* **2017**, *83*, 113–121. [CrossRef]
23. Nus, M.; Sage, A.P.; Lu, Y.; Masters, L.; Lam, B.Y.H.; Newland, S.; Weller, S.; Tsiantoulas, D.; Raffort, J.; Marcus, D.; et al. Marginal zone B cells control the response of follicular helper T cells to a high-cholesterol diet. *Nat. Med.* **2017**, *23*, 601–610. [CrossRef] [PubMed]
24. Nus, M.; Basatemur, G.; Galan, M.; Cros-Brunsó, L.; Zhao, T.X.; Masters, L.; Harrison, J.; Figg, N.; Tsiantoulas, D.; Geissmann, F.; et al. NR4A1 Deletion in Marginal Zone B Cells Exacerbates Atherosclerosis in Mice—Brief Report. *Arter. Thromb. Vasc. Biol.* **2020**, *40*, 2598–2604. [CrossRef] [PubMed]
25. Schmidt, A.; Oberle, N.; Krammer, P.H. Molecular Mechanisms of Treg-Mediated T Cell Suppression. *Front. Immunol.* **2012**, *3*, 51. [CrossRef]
26. Chagnon-Choquet, J.; Fontaine, J.; Poudrier, J.; Roger, M.; for the Montreal Primary HIV Infection and Slow Progressor Study Groups. IL-10 and Lymphotoxin-α Expression Profiles within Marginal Zone-Like B-Cell Populations Are Associated with Control of HIV-1 Disease Progression. *PLoS ONE* **2014**, *9*, e101949. [CrossRef]
27. Saze, Z.; Schuler, P.J.; Hong, C.-S.; Cheng, D.; Jackson, E.K.; Whiteside, T.L. Adenosine production by human B cells and B cell–mediated suppression of activated T cells. *Blood* **2013**, *122*, 9–18. [CrossRef]
28. Mackay, F.; Woodcock, S.A.; Lawton, P.; Ambrose, C.; Baetscher, M.; Schneider, P.; Tschopp, J.; Browning, J. Mice Transgenic for Baff Develop Lymphocytic Disorders along with Autoimmune Manifestations. *J. Exp. Med.* **1999**, *190*, 1697–1710. [CrossRef]
29. Hanna, Z.; Kay, D.G.; Cool, M.; Jothy, S.; Rebai, N.; Jolicoeur, P. Transgenic Mice Expressing Human Immunodeficiency Virus Type 1 in Immune Cells Develop a Severe AIDS-Like Disease. *J. Virol.* **1998**, *72*, 121–132. [CrossRef]
30. Hanna, Z.; Kay, D.G.; Rebai, N.; Guimond, A.; Jothy, S.; Jolicoeur, P. Nef Harbors a Major Determinant of Pathogenicity for an AIDS-like Disease Induced by HIV-1 in Transgenic Mice. *Cell* **1998**, *95*, 163–175. [CrossRef]
31. Steri, M.; Orrù, V.; Idda, M.L.; Pitzalis, M.; Pala, M.; Zara, I.; Sidore, C.; Faà, V.; Floris, M.; Deiana, M.; et al. Overexpression of the Cytokine BAFF and Autoimmunity Risk. *N. Engl. J. Med.* **2017**, *376*, 1615–1626. [CrossRef]
32. Nakayamada, S.; Tanaka, Y. BAFF- and APRIL-targeted therapy in systemic autoimmune diseases. *Inflamm. Regen.* **2016**, *36*, 1–6. [CrossRef]
33. Borhis, G.; Trovato, M.; Chaoul, N.; Ibrahim, H.; Richard, Y. B-Cell-Activating Factor and the B-Cell Compartment in HIV/SIV Infection. *Front. Immunol.* **2017**, *8*, 1338. [CrossRef]
34. Sintes, J.; Gentile, M.; Zhang, S.; Garcia-Carmona, Y.; Magri, G.; Cassis, L.; Segura-Garzón, D.; Ciociola, A.; Grasset, E.K.; Bascones, S.; et al. mTOR intersects antibody-inducing signals from TACI in marginal zone B cells. *Nat. Commun.* **2017**, *8*, 1462. [CrossRef]
35. Yi, Z.; Lin, W.W.; Stunz, L.L.; Bishop, G.A. Roles for TNF-receptor associated factor 3 (TRAF3) in lymphocyte functions. *Cytokine Growth Factor Rev.* **2013**, *25*, 147–156. [CrossRef]
36. Mambetsariev, N.; Lin, W.W.; Stunz, L.L.; Hanson, B.M.; Hildebrand, J.M.; Bishop, G.A. Nuclear TRAF3 is a negative regulator of CREB in B cells. *Proc. Natl. Acad. Sci. USA* **2016**, *113*, 1032–1037. [CrossRef]
37. Volakakis, N.; Kadkhodaei, B.; Joodmardi, E.; Wallis, K.; Panman, L.; Silvaggi, J.; Spiegelman, B.M.; Perlmann, T. NR4A orphan nuclear receptors as mediators of CREB-dependent neuroprotection. *Proc. Natl. Acad. Sci. USA* **2010**, *107*, 12317–12322. [CrossRef]
38. Bridi, M.S.; Hawk, J.D.; Chatterjee, S.; Safe, S.; Abel, T. Pharmacological Activators of the NR4A Nuclear Receptors Enhance LTP in a CREB/CBP-Dependent Manner. *Neuropsychopharmacology* **2016**, *42*, 1243–1253. [CrossRef]
39. Wen, A.Y.; Sakamoto, K.M.; Miller, L.S. The Role of the Transcription Factor CREB in Immune Function. *J. Immunol.* **2010**, *185*, 6413–6419. [CrossRef]
40. Safe, S.; Jin, U.H.; Morpurgo, B.; Abudayyeh, A.; Singh, M.; Tjalkens, R.B. Nuclear receptor 4A (NR4A) family—orphans no more. *J. Steroid Biochem. Mol. Biol.* **2016**, *157*, 48–60. [CrossRef]
41. Boudreaux, S.P.; Duren, R.P.; Call, S.G.; Nguyen, L.; Freire, P.R.; Narayanan, P.; Redell, M.S.; Conneely, O.M. Drug targeting of NR4A nuclear receptors for treatment of acute myeloid leukemia. *Leukemia* **2018**, *33*, 52–63. [CrossRef]
42. Deutsch, A.J.A.; Angerer, H.; Fuchs, T.E.; Neumeister, P. The nuclear orphan receptors NR4A as therapeutic target in cancer therapy. *Anti-Cancer Agents Med. Chem.* **2012**, *12*, 1001–1014. [CrossRef] [PubMed]

43. Antonioli, L.; Pacher, P.; Vizi, E.S.; Haskó, G. CD39 and CD73 in immunity and inflammation. *Trends Mol. Med.* **2013**, *19*, 355–367. [CrossRef] [PubMed]
44. Chang, W.X.; Huang, H.H.; Huang, L.; Shi, J.J.; Jiao, Y.M.; Zhang, C.; Jin, L.; Yang, T.; Shi, M.; Tu, B.; et al. Skewed CD39/CD73/adenosine pathway in B cells is associated with innate immune hyperactivation in chronic HIV-1 infection. *Transl. Med. Commun.* **2019**, *4*, 4. [CrossRef]
45. Kim, E.-S.; Ackermann, C.; Tóth, I.; Dierks, P.; Eberhard, J.M.; Wroblewski, R.; Scherg, F.; Geyer, M.; E Schmidt, R.; Beisel, C.; et al. Down-regulation of CD73 on B cells of patients with viremic HIV correlates with B cell activation and disease progression. *J. Leukoc. Biol.* **2017**, *101*, 1263–1271. [CrossRef]
46. Rothan, C.; Yero, A.; Shi, T.; Farnos, O.; Chartrand-Lefebvre, C.; El-Far, M.; Costiniuk, C.T.; Tsoukas, C.; Tremblay, C.; Durand, M.; et al. Antiretroviral therapy-treated HIV-infected adults with coronary artery disease are characterized by a distinctive regulatory T-cell signature. *AIDS* **2021**, *35*, 1003–1014. [CrossRef]
47. Zhou, S.N.; Zhang, N.; Liu, H.H.; Xia, P.; Zhang, C.; Song, J.W.; Fan, X.; Shi, M.; Jin, L.; Zhang, J.Y.; et al. Skewed CD39/CD73/adenosine pathway contributes to B-cell hyperactivation and disease progression in patients with chronic hepatitis B. *Gastroenterol. Rep.* **2020**, *9*, 49–58. [CrossRef]
48. Crean, D.; Cummins, E.P.; Bahar, B.; Mohan, H.; McMorrow, J.P.; Murphy, E.P. Adenosine Modulates NR4A Orphan Nuclear Receptors to Attenuate Hyperinflammatory Responses in Monocytic Cells. *J. Immunol.* **2015**, *195*, 1436–1448. [CrossRef]
49. Allard, B.; Allard, D.; Buisseret, L.; Stagg, J. The adenosine pathway in immuno-oncology. *Nat. Rev. Clin. Oncol.* **2020**, *17*, 611–629. [CrossRef]
50. Piper, C.J.; Rosser, E.C.; Oleinika, K.; Nistala, K.; Krausgruber, T.; Rendeiro, A.; Banos, A.; Drozdov, I.; Villa, M.; Thomson, S.; et al. Aryl Hydrocarbon Receptor Contributes to the Transcriptional Program of IL-10-Producing Regulatory B Cells. *Cell Rep.* **2019**, *29*, 1878–1892.e7. [CrossRef]
51. Poudrier, J.; Weng, X.; Kay, D.G.; Hanna, Z.; Jolicoeur, P. The AIDS-Like Disease of CD4C/Human Immunodeficiency Virus Transgenic Mice Is Associated with Accumulation of Immature CD11bHi Dendritic Cells. *J. Virol.* **2003**, *77*, 11733–11744. [CrossRef]
52. Louis, K.; Bailly, E.; Macedo, C.; Lau, L.; Ramaswami, B.; Chang, A.; Chandran, U.; Landsittel, D.; Gu, X.; Chalasani, G.; et al. T-bet+CD27+CD21− B cells poised for plasma cell differentiation during antibody-mediated rejection of kidney transplants. *JCI Insight* **2021**, *6*, e148881. [CrossRef] [PubMed]
53. Austin, J.W.; Buckner, C.M.; Kardava, L.; Wang, W.; Zhang, X.; Melson, V.A.; Swanson, R.G.; Martins, A.J.; Zhou, J.Q.; Hoehn, K.B.; et al. Overexpression of T-bet in HIV infection is associated with accumulation of B cells outside germinal centers and poor affinity maturation. *Sci. Transl. Med.* **2019**, *11*, eaax0904. [CrossRef]
54. Knox, J.J.; Kaplan, D.E.; Betts, M.R. T-bet-expressing B cells during HIV and HCV infections. *Cell. Immunol.* **2017**, *321*, 26–34. [CrossRef] [PubMed]
55. Woodruff, M.C.; Ramonell, R.P.; Nguyen, D.C.; Cashman, K.S.; Saini, A.S.; Haddad, N.S.; Ley, A.M.; Kyu, S.; Howell, J.C.; Ozturk, T.; et al. Extrafollicular B cell responses correlate with neutralizing antibodies and morbidity in COVID-19. *Nat. Immunol.* **2020**, *21*, 1506–1516. [CrossRef] [PubMed]
56. Knox, J.J.; Buggert, M.; Kardava, L.; Seaton, K.E.; Eller, M.; Canaday, D.H.; Robb, M.L.; Ostrowski, M.A.; Deeks, S.G.; Slifka, M.K.; et al. T-bet+ B cells are induced by human viral infections and dominate the HIV gp140 response. *JCI Insight* **2017**, *2*, e92943. [CrossRef]
57. Mauri, C. Novel Frontiers in Regulatory B cells. *Immunol. Rev.* **2021**, *299*, 5–9. [CrossRef]
58. Attanavanich, K.; Kearney, J.F. Marginal Zone, but Not Follicular B Cells, Are Potent Activators of Naive CD4 T Cells. *J. Immunol.* **2004**, *172*, 803–811. [CrossRef]
59. Cinamon, G.; Zachariah, M.A.; Lam, O.M.; Foss, F.W.; Cyster, J.G. Follicular shuttling of marginal zone B cells facilitates antigen transport. *Nat. Immunol.* **2008**, *9*, 54–62. [CrossRef]
60. Bialecki, E.; Paget, C.; Fontaine, J.; Capron, M.; Trottein, F.; Faveeuw, C. Role of Marginal Zone B Lymphocytes in Invariant NKT Cell Activation. *J. Immunol.* **2009**, *182*, 6105–6113. [CrossRef]
61. Doyon-Laliberté, K.; Aranguren, M.; Poudrier, J.; Roger, M. Marginal Zone B-Cell Populations and Their Regulatory Potential in the Context of HIV and Other Chronic Inflammatory Conditions. *Int. J. Mol. Sci.* **2022**, *23*, 3372. [CrossRef]
62. Mercier, F.; Boulassel, M.R.; Yassine-Diab, B.; Tremblay, C.; Bernard, N.F.; Sekaly, R.P.; Routy, J.P. Persistent human immunodeficiency virus-1 antigenaemia affects the expression of interleukin-7Ralpha on central and effector memory CD4+ and CD8+ T cell subsets. *Clin. Exp. Immunol.* **2008**, *152*, 72–80. [CrossRef] [PubMed]
63. Love, M.I.; Huber, W.; Anders, S. Moderated estimation of fold change and dispersion for RNA-seq data with DESeq2. *Genome Biol.* **2014**, *15*, 550. [CrossRef] [PubMed]
64. Subramanian, A.; Tamayo, P.; Mootha, V.K.; Mukherjee, S.; Ebert, B.L.; Gillette, M.A.; Paulovich, A.; Pomeroy, S.L.; Golub, T.R.; Lander, E.S.; et al. Gene set enrichment analysis: A knowledge-based approach for interpreting genome-wide expression profiles. *Proc. Natl. Acad. Sci. USA* **2005**, *102*, 15545–15550. [CrossRef] [PubMed]
65. Mootha, V.K.; Lindgren, C.M.; Eriksson, K.-F.; Subramanian, A.; Sihag, S.; Lehar, J.; Puigserver, P.; Carlsson, E.; Ridderstråle, M.; Laurila, E.; et al. PGC-1α-responsive genes involved in oxidative phosphorylation are coordinately downregulated in human diabetes. *Nat. Genet.* **2003**, *34*, 267–273. [CrossRef] [PubMed]